



Preclinical characterization of NVL-330, a selective and brain penetrant HER2 tyrosine kinase inhibitor with broad activity on HER2 oncogenic alterations

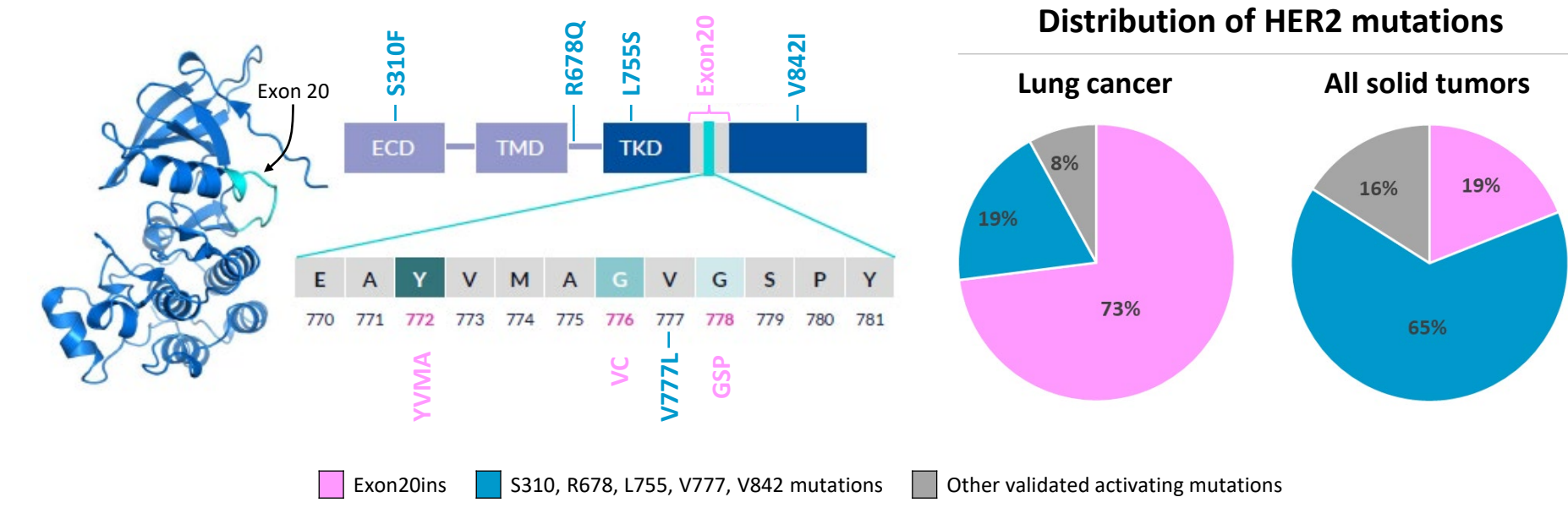
Yuting Sun¹, Kristin L. Andrews¹, Anupong Tangpeerachaikul¹, Tuan M. Nguyen¹, Baudouin Gerard¹, Nancy E. Kohl², Joshua C. Horan¹, Henry E. Pelish¹

¹Nuvalent, Cambridge, MA; ²Kohl Consulting, Wellesley, MA

ADDRESSING A MEDICAL NEED

HER2 Oncogenic Mutations

- HER2 (ERBB2) can drive tumorigenesis via mutation, amplification, and/or overexpression.¹
- HER2 exon 20 insertion mutations (exon20ins) induce constitutive kinase activity and are the most frequently occurring HER2 mutations in lung cancer. Examples include Y772_A775dupYVMA (HER2^{YVMA}), G776del_insVC (HER2^{VC}), and P780_Y781insGSP (HER2^{GSP}).¹⁻³
- In all solid tumors, point mutations at five hotspots (S310, R678, L755, V777, and V842) account for ~65% of HER2 mutations.²



▲ Figure 1 (Left) Schematic illustration showing locations of major oncogenic mutations on HER2 protein (PDB: 7JXH). (Right) Pie charts showing the distribution of HER2 mutations in NSCLC and all solid tumors.²

HER2-mutant NSCLC Landscape

- Antibody drug conjugate trastuzumab deruxtecan (T-DXd; Enhertu®) has received accelerated approval for previously treated HER2-mutant non-small cell lung cancer (NSCLC), with intracranial activity reported.⁴⁻⁵
- Selective HER2 tyrosine kinase inhibitor (TKI) zongertinib has demonstrated preliminary clinical activity in HER2-mutant NSCLC.⁶ Its intracranial activity has not been reported.
- Additional HER2-selective or EGFR/HER2-targeting TKIs are under clinical development.

NVL-330 Preclinical Profile⁷

- Activity against oncogenic HER2 mutants and wild-type HER2**
 - 2 – 4% of NSCLC patients have HER2 oncogenic mutations.⁸⁻⁹
 - 1 – 5% of NSCLC patients have HER2 amplifications.⁸⁻⁹
- Sparing wild-type EGFR, to mitigate adverse events and dose-limiting toxicities associated with wild-type EGFR inhibition**

Inhibition of the closely related ERBB family member wild-type EGFR is associated with adverse events including skin rash and diarrhea.
- Activity in the central nervous system (CNS)**

Almost 50% of HER2-mutant metastatic NSCLC patients develop brain metastases.¹⁰

> Abbreviations: amp, amplification; BID, twice per day; CNS, central nervous system; ECD, extra-cellular domain; Exon20ins, exon 20 insertion mutations; HP-β-CD, 2-Hydroxypropyl-β-cyclodextrin; IV, intravenously; Kp, brain-to-plasma partitioning coefficient; Kp_{uu}, unbound brain-to-plasma partitioning coefficient; MPAS, MAPK pathway activity score; NIH, National Institute of Health; NSCLC, non-small cell lung cancer; PBS, phosphate buffered saline; PDX, patient derived xenograft; phospho-EGFR, phosphorylated EGFR; phospho-HER2, phosphorylated HER2; PO, orally; Q3W, once every three weeks; SEM, standard error of the mean; T-DXd, trastuzumab deruxtecan; T-DXd-R, T-DXd resistant; TKD, tyrosine kinase domain; TKI, tyrosine kinase inhibitor; TMD, transmembrane domain; WT, wild-type.

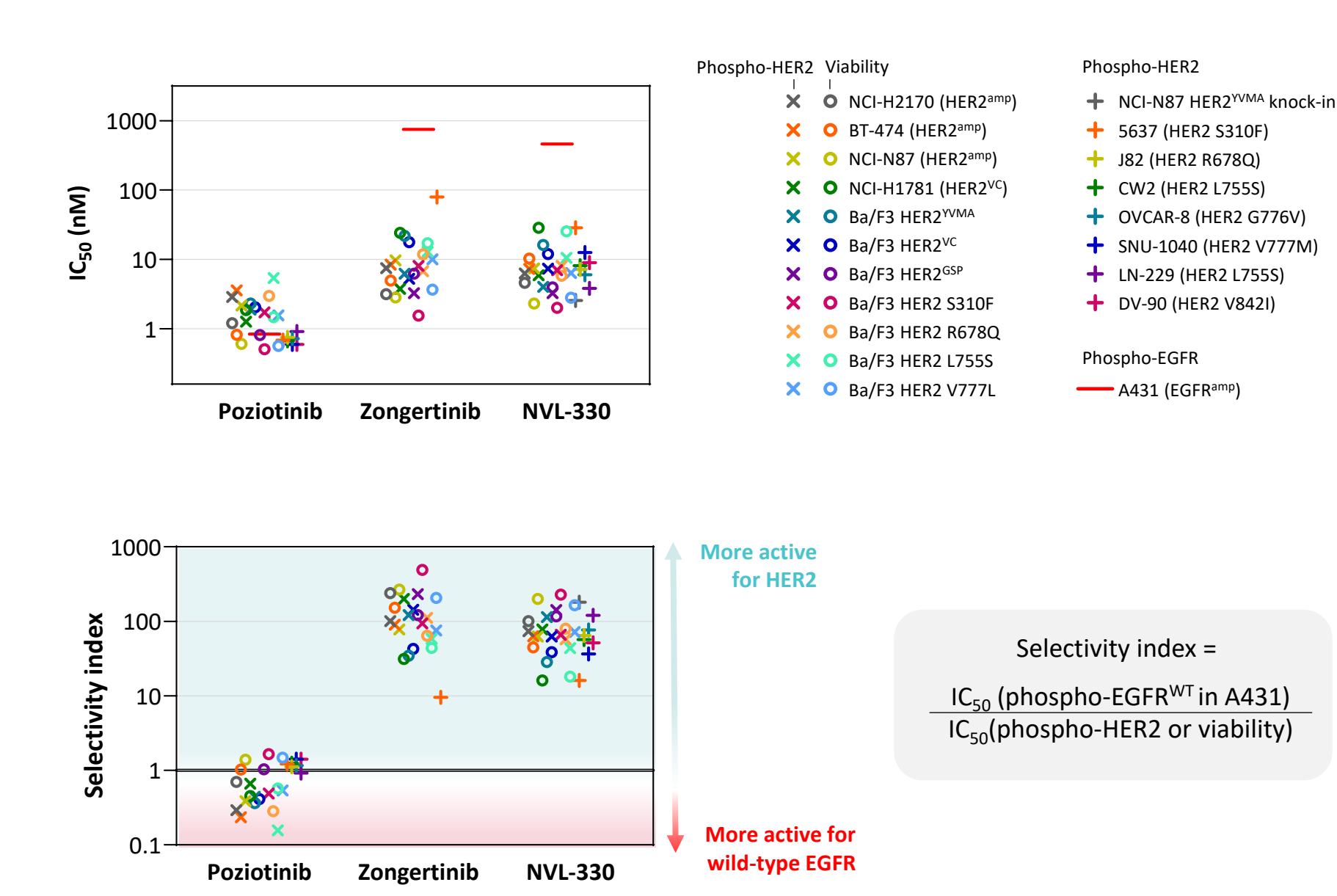
> References
¹Robichaux et al., *Cancer Cell* 2019
²Ishiyama et al., *Cancer Research* 2022
³Perera et al., *PNAS* 2009
⁴FDA Prescribing Information (Reference ID: 5029058)
⁵Li et al., *ESMO Conference* 2023
⁶Yamamoto et al., *IASLC World Conference of Lung* 2022
⁷Andrews et al., *EORTC-NCI-AACR Conference* 2022
⁸Li et al., *J Thoracic Oncology* 2016
⁹Liu et al., *Clinical Cancer Research* 2018
¹⁰Offin et al., *Cancer* 2019
¹¹Shaw et al., *NEJM* 2020
¹²Wagle et al., *NPI Precision Oncology* 2018
¹³Wang et al., *SITC Conference* 2023

> Financial Disclosures: YS, KLA, AT, TMN, BG, JCH and HEP are employees and shareholders of Nuvalent, Inc. NEK is a consultant of Nuvalent, Inc.
 > Disclaimer: Head-to-head clinical studies comparing NVL-330 with currently approved or investigational therapies have not been conducted.

IN VITRO POTENCY AND SELECTIVITY

NVL-330: a Broadly Active and Selective HER2 TKI

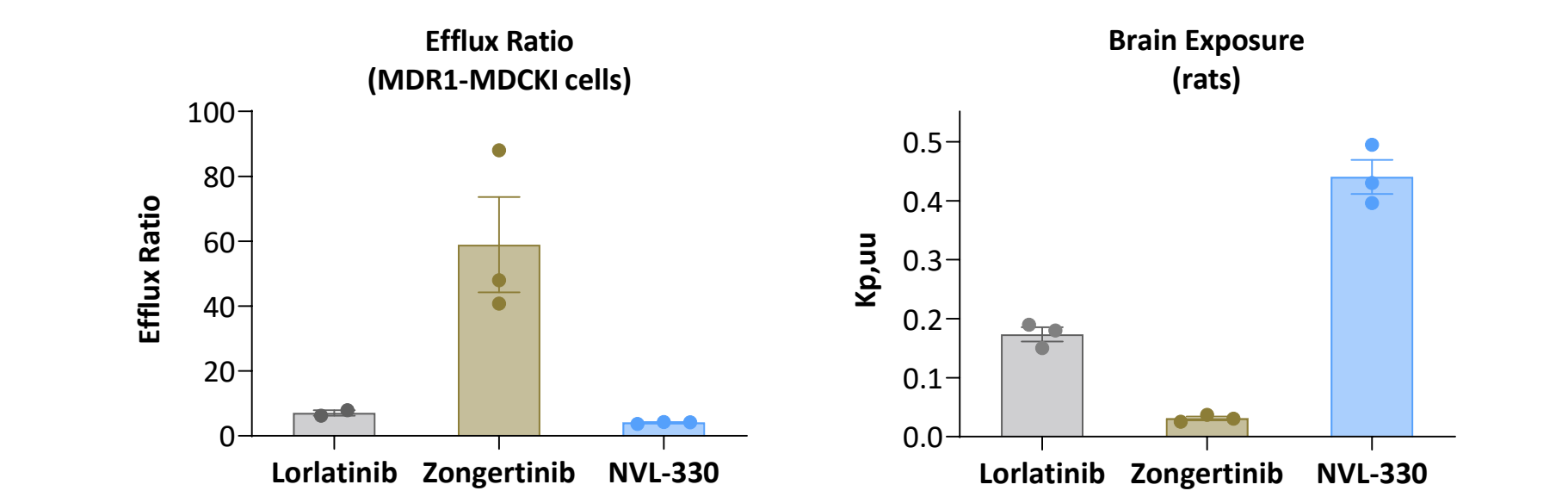
- NVL-330 showed broad activity on HER2 oncogenic alterations, including HER2 exon20ins, activating point mutations, and amplified wild-type HER2.
- NVL-330 and zongertinib had similar HER2 potency and selectivity over wild-type EGFR.
- Pozitotinib, a pan-ERBB inhibitor, did not demonstrate selectivity over wild-type EGFR.



▲ Figure 2 (Top) IC₅₀ values of NVL-330 in phospho-HER2 or phospho-EGFR AlphaLISA® assays or CellTiter-Glo® viability assays. (Bottom) Selectivity indexes over wild-type EGFR as defined by the formula in the graph. AlphaLISA® assays were conducted after a 4-hour treatment. CellTiter-Glo® viability assays were conducted after a 2-day (Ba/F3), 5-day (NCI-H1781), or 3-day (all other cell lines) treatment. The phospho-EGFR assay in A431 cells was conducted without EGF. The phospho-HER2 assay in 5637 cells was conducted with 30 ng/mL EGF. The NCI-N87 HER2^{YVMA} knock-in cell line was generated via CRISPR/Cas9. Geometric means plotted (n = 2 – 51, except n=1 for the following: pozitotinib in NCI-H2170 phospho-HER2, zongertinib in BT-474 phospho-HER2, and zongertinib in NCI-H2170 viability assays).

CNS PENETRATION

- Low efflux (measured in the MDR1-MDCK1 cells) and high brain-to-plasma partitioning (measured by rat Kp_{uu}) are positive predictors of brain exposure in humans.
- NVL-330 had an efflux ratio and Kp_{uu} comparable to lorlatinib, a CNS-active TKI benchmark.¹¹
- Zongertinib had a high efflux ratio and a low Kp_{uu}.

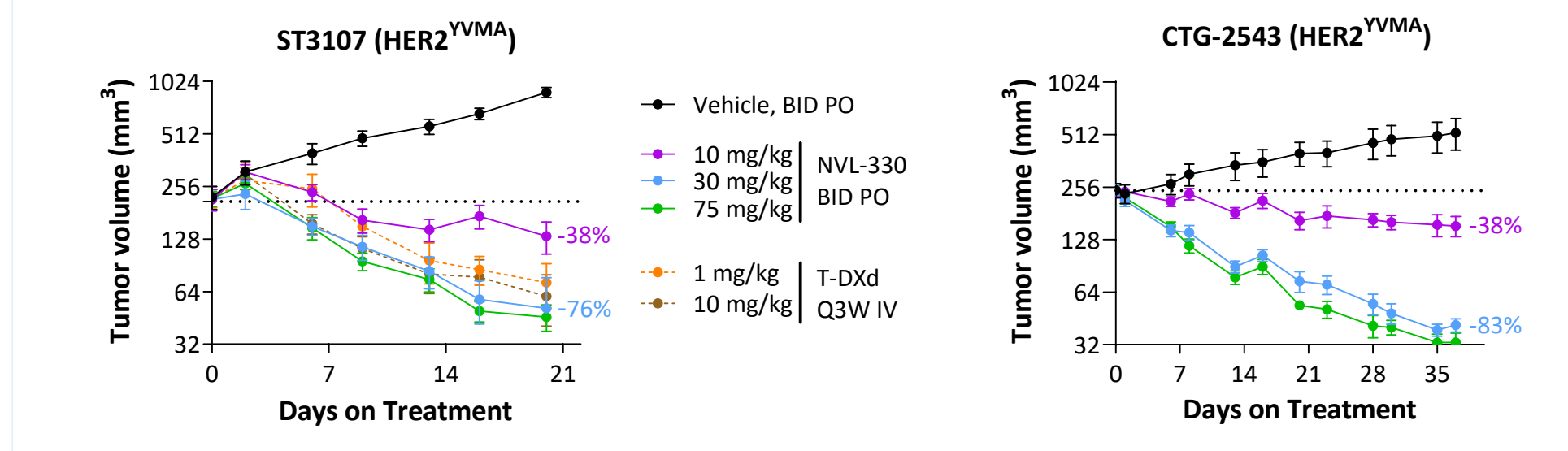


▲ Figure 3 (Left) Efflux ratio defined as P_{app}(B-A)/P_{app}(A-B) in MDR1-MDCK1 cells (NIH; n = 2 – 3). (Right) Unbound brain-to-plasma partitioning coefficient (Kp_{uu}) determined at 1 hour after a single oral dose of 10 mg/kg of lorlatinib, zongertinib or NVL-330 in Wistar Han rats (n = 3), adjusted for fraction unbound in rat plasma and brain homogenate. Average ± SEM plotted.

IN VIVO ANTITUMOR ACTIVITY

Activity in HER2 Exon20ins PDX Models

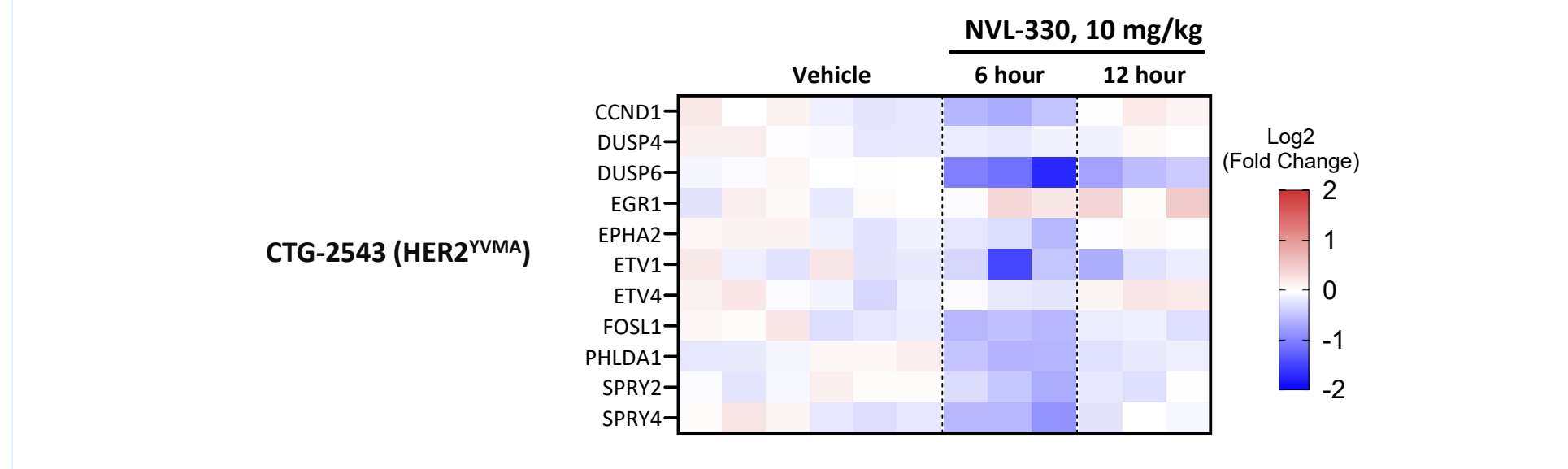
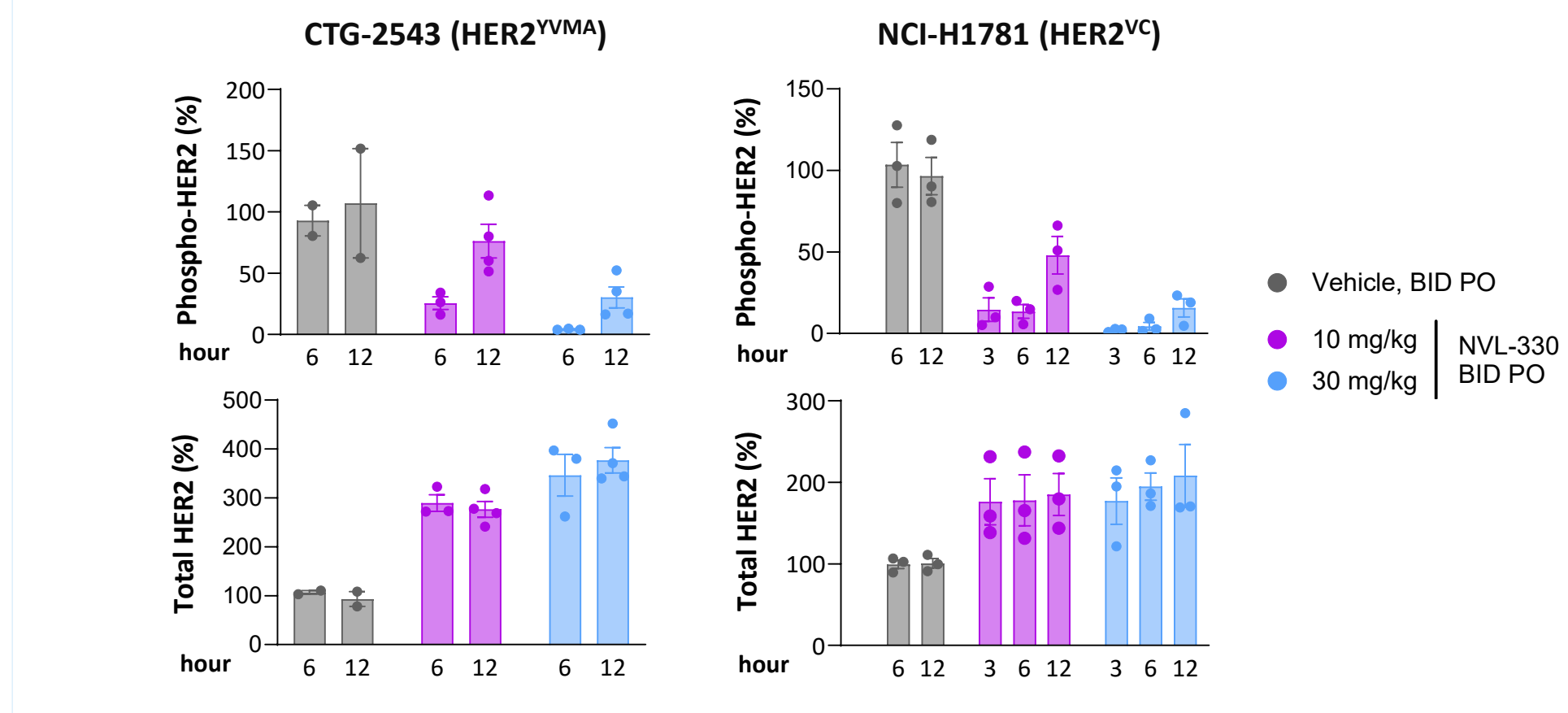
- NVL-330 showed dose-dependent antitumor efficacy in patient derived xenograft (PDX) models harboring HER2^{YVMA}, with regression starting at 10 mg/kg BID PO.
- T-DXd achieved tumor regression in the ST3107 model.



▲ Figure 4 Antitumor activity in subcutaneous ST3107 (Left) and CTG-2543 (Right) NSCLC PDX models in mice. Vehicle was 20% HP-β-CD pH=3 – 3.5 for NVL-330. T-DXd was diluted in PBS before IV administration. Average tumor volume changes for NVL-330 treated mice (10 and 30 mg/kg) compared to baseline are annotated. All treatments were well tolerated, without significant body weight loss. Average ± SEM plotted (n = 5 mice per group; n = 4 after day 20 for 10 mg/kg NVL-330 group in the CTG-2543 model).

Pharmacodynamic Activity

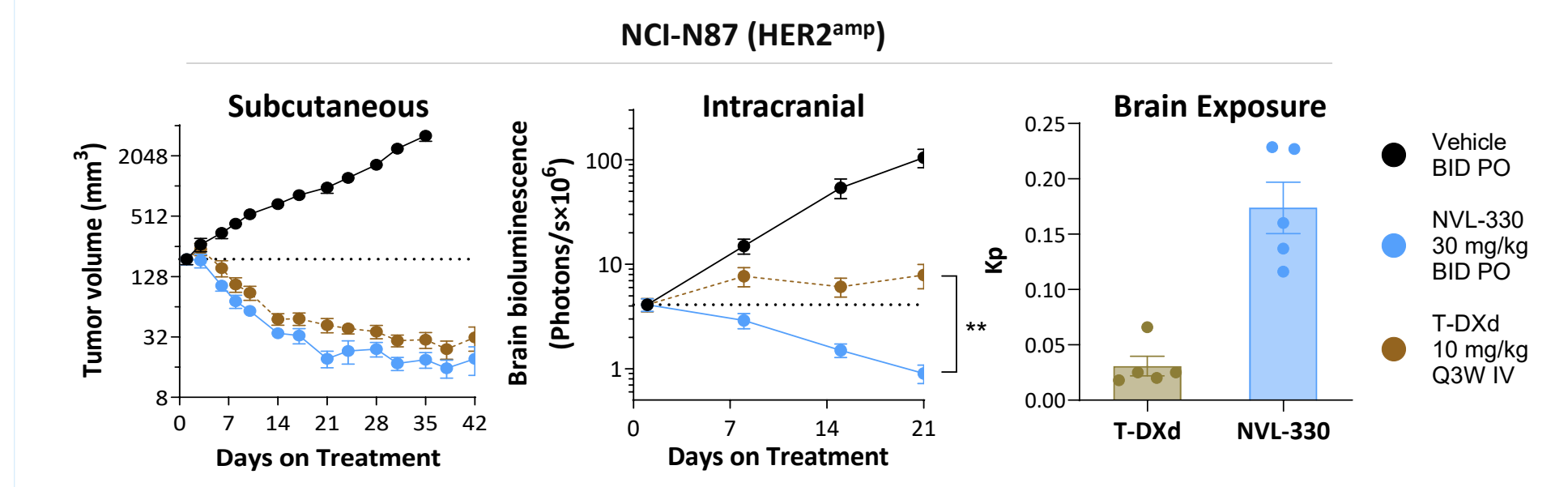
- NVL-330 suppressed phospho-HER2 and increased total HER2 in CTG-2543 (HER2^{YVMA}) and NCI-H1781 (HER2^{VC}) tumors.
- NVL-330 suppressed downstream MAPK pathway activity, as measured by reductions in mRNA levels of DUSP6 and other MAPK pathway activity score (MPAS) genes.¹²



▲ Figure 5 Pharmacodynamic analyses in CTG-2543 and NCI-H1781 tumor samples collected from mice after 3-day treatment with vehicle or NVL-330. (Top) MSD analysis of phospho-HER2 Y1248 and total HER2 in tumors collected at multiple time points after the final dose, plotted as percent of average of vehicle. (Bottom) Changes in MPAS gene transcript levels in CTG-2543 tumors determined by RNA-seq. Each column represents one mouse. Vehicle treated tumors collected at 6-hour and 12-hour were combined as one group in data analysis.

Intracranial Activity of NVL-330 and T-DXd

- NVL-330 (30 mg/kg BID) induced subcutaneous and intracranial NCI-N87 tumor regression.
- T-DXd (10 mg/kg Q3W, a clinically relevant dose in mice) induced NCI-N87 tumor stasis intracranially, despite subcutaneous tumor regression.
- NVL-330 demonstrated higher brain penetrance than T-DXd at the intracranial study endpoint.

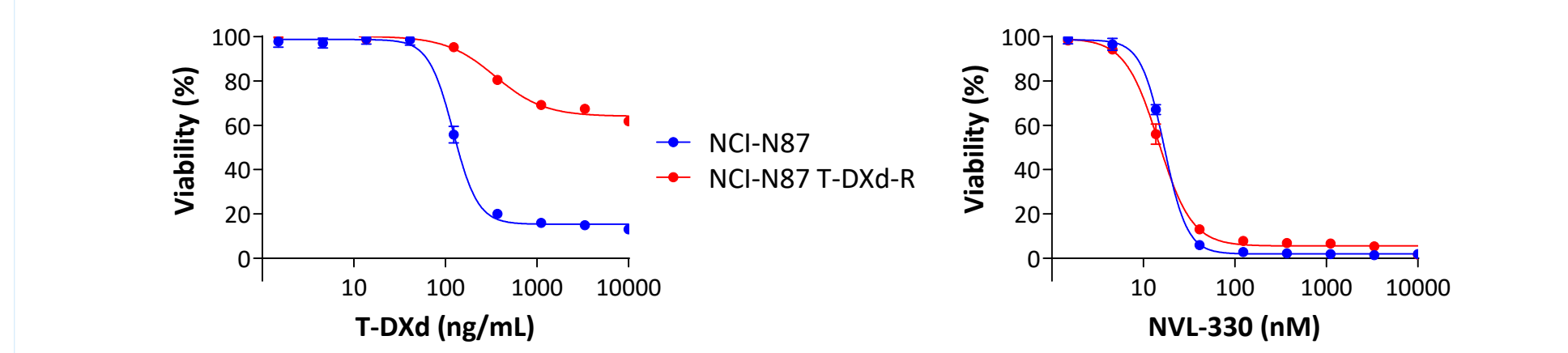


▲ Figure 6 Antitumor activity in NCI-N87-Luc subcutaneous (Left, n = 5) and intracranial (Middle, n = 10 – 18) tumor models in nude mice. Intracranial tumor burden was assessed by bioluminescence imaging. The treatment started 12 days after intracranial tumor implantation. Statistical analysis was conducted using 2-way ANOVA with the Geisser-Greenhouse correction. **, p < 0.01. (Right) Brain-to-plasma partitioning coefficient (Kp) from mice on day 21 at the dosing trough in the intracranial study. N=5. Average ± SEM plotted.

ACTIVITY POST T-DXd

NVL-330 Activity Following T-DXd Acquired Resistance

- The T-DXd resistant cell line (NCI-N87 T-DXd-R) was generated via long-term culturing of NCI-N87 cells with T-DXd, which resulted in payload (DX-8951 derivative) resistance.¹³
- NVL-330 was equally effective in NCI-N87 and NCI-N87 T-DXd-R cells in vitro.



▲ Figure 7 Dose response curves of NCI-N87 and NCI-N87 T-DXd-R cells towards T-DXd (Left) and NVL-330 (Right) determined in a 6-day CellTiter-Glo® viability assay. Average ± SEM plotted (n = 6, from two independent experiments).

CONCLUSIONS

- NVL-330 had broad preclinical activity on HER2 oncogenic alterations, including HER2 exon20ins, HER2 activating point mutations, and amplified wild-type HER2.
- Preclinical comparison with zongertinib
 - Similar potency and selectivity over wild-type EGFR;
 - NVL-330 demonstrated higher CNS penetrance.
- Preclinical comparison with T-DXd
 - NVL-330 achieved deeper response and higher CNS penetrance in an intracranial tumor model;
 - NVL-330 had activity in cells with acquired resistance to T-DXd.
- Initiation of a Phase 1 clinical trial for NVL-330 is planned in 2024.

